Nanostructure and Thermal Stability of the Polyglutamate Langmuir−Blodgett Films Probed by Interlayer Energy Transfer Method

Michiaki Mabuchi, Shinzaburo Ito,* Masahide Yamamoto, and Takeaki Miyamoto†

Department of Polymer Chemistry, Graduate School of Engineering, Kyoto University, Yoshida, Sakyo, Kyoto 606-8501, Japan

Albert Schmidt and Wolfgang Knoll

Max-Planck-Institut für Polymerforschung, Ackermannweg 10, D-55128 Mainz, Germany

Received July 6, 1998; Revised Manuscript Received October 19, 1998

ABSTRACT: Ultrathin films of α-helical polyglutamate with long flexible side chains (PG) were fabricated by the LB technique, and their nanostructure was investigated by the energy transfer method. The rodlike main chain of PG was labeled by incorporating either energy donor (naphthalene, Np) or acceptor (anthracene, An) molecules via short side chains. The fluorescence spectra of Np−An multilayers with the same number of spacing layers gave different energy transfer efficiencies, depending on the mode of depositions. This phenomenon was interpreted as being caused by the noncentered structure of the polymer backbone, which was probed by both X-ray reflectometry and fluorescence spectroscopy. The Y-type deposition induced a bilayer structure in which the stiff main chains of each monolayer were located close to the center of the bilayer. The layered structures showed excellent thermal stability up to around 120 °C. By thermal treatment higher than 120 °C, the layered structure relaxed to a stable state in which the α-helical backbones in each layer became intermingled.

Introduction

To control photoprocesses such as excited energy transfer and photoinduced electron transfer, functional molecules need to be placed in a restricted molecular geometry. The LB technique is one of the most powerful methods to organize a highly ordered molecular assembly under mild conditions. Polymeric LB films are more promising materials for the application to photofunctional devices than the conventional LB films of low molecular weight amphiphiles because of their unique properties; the introduction of a small content of functional groups into the polymer chain enables uniform dispersion of the groups without aggregation; and thinness of the monolayer (0.4−2 nm) is useful to control the spacing of the layered assemblies at nanometer dimensions.[1−6]

For further photofunctionality, the distance and orientation of functional molecules should be ordered more restrictedly. Recently, a new class of LB materials, "hairy-rod polymers", have been introduced and developed.[7,8] As illustrated in Figure 1, this macromolecule consists of two elements: a stiff backbone of the polymer main chain (rod) and a radial skin of the flexible alkyl side chains (hair). The former gives the well-defined macromolecular structure with rigidity, and the latter ensures solubility of the rigid-rod molecules and processability, e.g., the LB transfer to solid substrates. The LB films of these polymers have some unique characteristics such as preferential orientation of the rods to the dipping direction[9,10] and high thermal and mechanical stability.[11] Poly[(γ-methyl-L-glutamate)-*co*-(γ-octadecyl-L-glutamate)] with 30 mol % octadecyl unit (PG) is an excellent example of such polymers.[12,13] In the case of PG, an α-helical main chain of polypeptide forms the rigid backbone.

† Institute for Chemical Research.

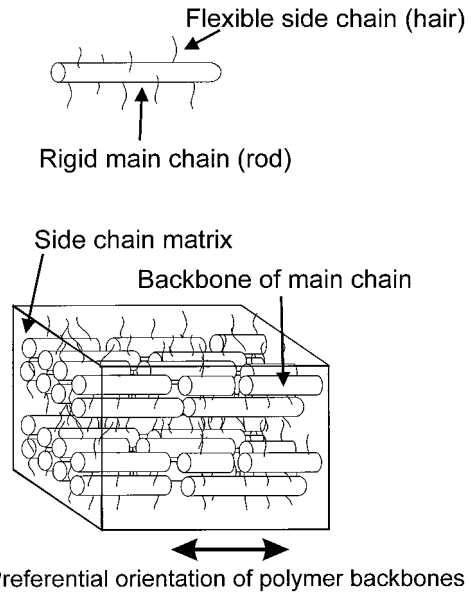

Figure 1. (top) Single molecule of "hairy-rod" polyglutamate. (bottom) Schematic illustration of a multilayer structure of the PG LB film.

The aim of the present study is to observe and characterize the inner structure of the LB film of this hairy-rod PG by the fluorescence technique. The chromophores incorporated into the polymer chain can act as a probe providing quantitative information about the nanostructure of the LB film because photophysical processes such as nonradiative singlet energy transfer occur at the scale of a few nanometers.[14,15] This allows for another approach for structural analysis, being different from X-ray or neutron reflectometry.[16,17] In this way the PG's having chromophores in the short side chain have been synthesized, and their LB assembly

10.1021/ma981050f CCC: $15.00
Published on Web 11/20/1998

Chart 1. Chemical Structure of PG Used in This Study

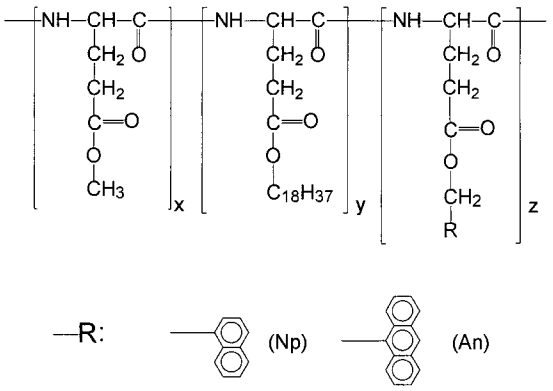

Table 1. Composition of PG's and Surface Pressures at LB Deposition

sample	*x* (%)	*y* (%)	*z* (%)	surf. press. of deposition (mN m^{-1})
PG	73.6	26.4	0	25
PG−Np[a]	61.6	23.3	15.1	20
PG−An[a]	70.8	27.7	1.50	20

[a] Chloroform containing approximately 1% trifluoroacetic acid was used as the spreading solvent.[18]

properties and fluorescence properties in LB films have been examined previously.[18] Herein, using these PG's as energy-donating/accepting polymers, the initial structure of the LB films and its thermal stability have been investigated by means of interlayer energy transfer measurement.

Experimental Section

Materials. Poly[(γ-methyl-L-glutamate)-*co*-(γ-octadecyl-L-glutamate)] derivatives with octadecyl units of 20−30 mol % were used. The chemical structure and compositions of the polymers are shown in Chart 1 and Table 1, respectively. The polymers were labeled with naphthalene (Np) and anthracene (An) chromophores as the energy-donating and -accepting groups, respectively. A set of the polymers were synthesized by triethylamine-initiated copolymerization of the corresponding *N*-carboxyanhydrides. The details of synthesis, characterization, and the monolayer behavior have been described elsewhere.[18] The condition used here for the NCA polymerization gives rise to polymers on the order of DP = 100. The molecular weight for the obtained samples was found to be in the range 10^4−10^5 by the GPC analysis using polystyrene standards. But the exact molecular weight was not measured, since molecular weight does not affect the LB deposition behavior and other structural properties of the resulting film for this type of polymer.[12b]

Fabrication of LB Films. A floatglass plate (25 mm × 75 mm, for X-ray reflectometry), a nonfluorescent quartz plate (10 mm × 40 mm, for the energy transfer measurement), and a silicon substrate (10 mm × 40 mm, for FT-IR measurement) were used as substrates. These substrates were cleaned in oxidative sulfuric acid, rinsed with pure water, and then made hydrophobic by dipping in a 10% solution of trimethylchlorosilane in toluene. The polymers were spread from a chloroform solution[19] (0.3 wt %) on the Teflon-coated trough (Kenkosha model SI-1) filled with ultrapure water (Barnstead Nanopure II). After left to stand for 15 min, the monolayer film was compressed at 10 mm min^{-1} to the given surface pressure shown in Table 1. After the surface area was stabilized at this pressure, the deposition was carried out by dipping/raising the substrate vertically at a rate of 15 mm min^{-1}. The surface pressure−area isotherm and the deposition behavior did not depend on the introduction of the chromophores up to 15 mol %. The temperature of the subphase was kept at 20 ± 0.2 °C throughout the process. The transfer ratio for all the samples was approximately unity in both the up and down modes, yielding a Y-type built-up film.

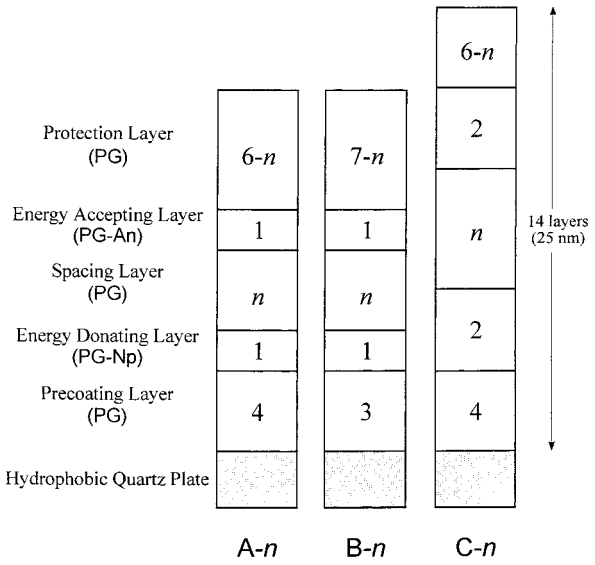

Figure 2. Schematic illustration of the layered structure of LB films for the energy transfer measurement. A-*n* and B-*n* are the samples to investigate the as-deposited structure, having different numbers of precoating layers. The character *n* is the number of spacing layers, 0 or 2. C-*n* is the sample to investigate the thermal stability of the layered structure.

Figure 2 schematically illustrates the structure of the LB films used for the energy transfer measurements. The sample films were fabricated on a quartz substrate in the following sequence: (1) PG layers for the precoating layers, (2) PG−Np layers for the energy-donating layers, (3) PG layers for the spacer between the energy-donating and the energy-accepting layers, (4) PG−An layers for the energy-accepting layers, and (5) PG layers for the surface-protecting layers. To investigate the initial structure of the film, the single layers of PG−Np and PG−An were deposited for the probing layers (see Figure 2). The samples whose number of precoating layers is 3 and 4 are abbreviated as A-*n* and B-*n*, respectively, where *n* is the number of spacing layers, 0 or 2. Since *n* is an even number and the monolayers were transferred by the Y-type deposition, the energy-donating layer is deposited on the downstroke dip and the accepting layer is deposited on the upstroke dip for the A-*n* samples, while vice versa for the B-*n* samples. In measuring the thermal stability of the layered structure, double layers of PG−Np and PG−An were deposited as the probing layers in order to obtain stronger fluorescence intensity (Figure 2). This sample is abbreviated as C-*n*, where *n* is also the number of spacing layers, 0, 2, and 4. To fix the composition of the film regardless of *n*, the total number of layers for C-*n* was kept constant at 14.

X-ray Reflectometry. X-ray reflectometry for the LB multilayers in specular reflection geometry was measured by a Philips PW1820 reflectometer. An 18 kW rotating anode with a graphite monochromator was used at a wavelength of 1.54 Å (Cu Kα radiation).[20] Reflectivity could be measured down to approximately 10^{-7}. All measurements were performed at room temperature.

FT-IR Spectroscopy. FT-IR measurements were performed on a Perkin-Elmer System-2000 FT-IR spectrometer. A reference spectrum of a freshly cleaned silicon substrate was recorded and used as a background spectrum. For thermal stability measurements, the sample film was heated to the desired temperature in a thermoregulated sample chamber for 20 min. After cooling to room temperature, the IR spectra were measured.

Fluorescence Spectroscopy. Fluorescence spectra of the multilayers were recorded by a Hitachi 850 spectrophotometer. The instrument was equipped with a thermoregulated sample

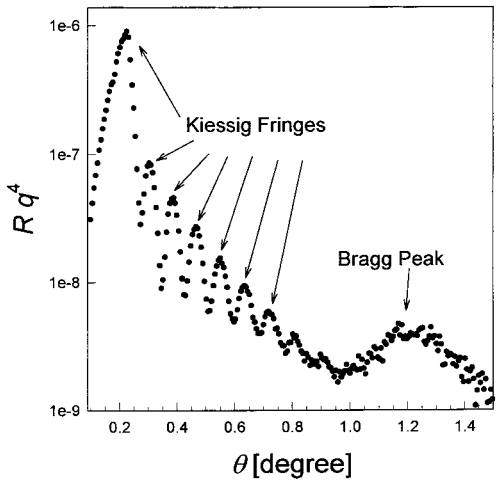

Figure 3. X-ray reflectivity curve of the PG−Np 20-layer film.

Table 2. Structural Parameters of the PG Multilayers Determined by X-ray Reflectometry

sample	no. of monolayers	Bragg peak spacing (nm)	thickness of total film (nm)	av. thickness per layer (nm)
PG	18	3.90	31.4 ± 0.2	$L = 1.74$
PG−Np	10	3.53	17.7 ± 0.2	$L_D = 1.77$
PG−An	10	3.53	17.6 ± 0.2	$L_A = 1.76$

chamber for the measurement of thermal stability. Heating and cooling rates were fixed to be 0.5 °C min^{-1} in the range 30−190 °C.

Results and Discussion

As-Deposited Structure Probed by X-ray Reflectometry. X-ray reflectometry in the specular reflection geometry was used to probe the microstructure of the ultrathin films along the film normal, z.[14,15,21−23] A typical example of the reflectivity curve for a PG−Np 20-layer film is shown in Figure 3. As the dominant features, Kiessig fringes as well as a Bragg peak were observed. The Bragg peak indicates a well-defined layer structure because it is a result of the internal periodic electron density. LB films of amorphous polymers, in general, do not show a Bragg peak because of the lack of the contrast of the electron density, whereas the high electron density in the polypeptide main chain gave a Bragg peak for the PG LB film. Analysis of the Bragg peak provides the length of the spacing for the internal periodic structure. The series of peaks on the reflectivity curve, referred to as Kiessig fringes, arise from the interference of the X-ray beam reflected from the air/film and from the film/substrate interface.[24] The total thickness of the film was evaluated from the spacing between the fringes. Table 2 shows the result of the X-ray reflectometry.

The periodicity of the layered structure determined from the Bragg peak was twice the average thickness of the monolayer. This means that the periodicity corresponds to a bilayer structure. This structure is also seen for LB films of other hairy-rod polymers,[7,8,12,13] a result of the Y-type deposition of the layers. The process is schematically depicted in Figure 4.

When a PG molecule is spread on a water surface, the stiff main chains are likely to lie flat on the surface. The hydrophobic alkyl side chains are stretched to the air side, whereas the backbone of the main chain with the hydrophilic peptide group comes close to the water phase.[25] Thus, the monolayer film of PG has a noncentered structure in which the stiff main chain is located near the water surface. This noncentered structure is retained after the deposition. In dipping the substrate for the vertical deposition, the monolayer is transferred to the hydrophobic substrate by contact with the upper side of the monolayer, while in lifting it is transferred by contact with the lower side. Consequently, the Y-type transfer yields the structure as shown in Figure 4 in which the stiff main chains are placed close to the center of each bilayer. This result for PG−Np and PG−An indicates that the attached chromophores did not influence the architecture of the PG assemblies. This is also supported by CD and polarized IR measurements; an α-helical main chain of PG−Np or PG−An in the LB film preferentially oriented to the dipping direction, as well as nonchromophoric PG.

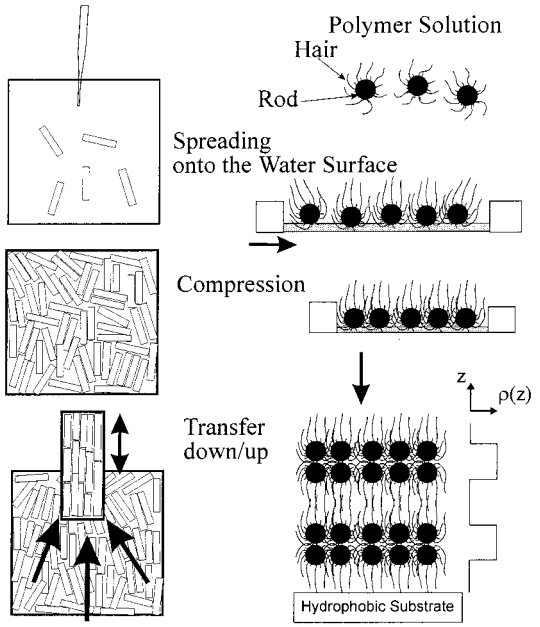

Figure 4. "Bilayer structure" formed in the PG LB film. $\rho(z)$ indicates the electron density in the film.

As-Deposited Structure Probed by the Energy Transfer Method. Since the rate of nonradiative singlet energy transfer is proportional to the −6th power of the distance between donor and acceptor molecules (r_{DA}), the energy transfer method is very sensitive to the alteration of the distance on a nanometer scale. Naphthalene−anthracene is one of the typical donor−acceptor pairs, and its Förster radius is 2.31 nm.[26] Figure 5 shows the fluorescence spectra of LB films, A-n and B-n, where the ordinate is normalized to the peak intensity of the Np emission. The Np chromophores were excited selectively at 283 nm. However, the fluorescence spectra showed both Np emission (328, 338 nm) and An emission (390, 415, 438 nm), indicating that interlayer energy transfer occurred. The fluorescence spectra of the multilayer film of PG−Np or PG−An showed only monomer emission without excimer emission,[18] revealing that Np or An chromophores were separated from each other.

The energy transfer efficiency depended on n; by increasing n, the intensity of Np increased and that of An decreased, indicating the decrease of the transfer efficiency. It should be noted that the transfer efficiencies for A-0 and B-0 were different from each other, as shown in Figure 5. This implies that r_{DA} of these two samples are different despite the same number of

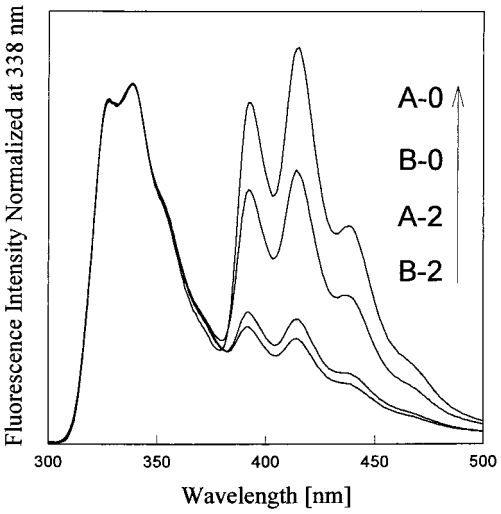

Figure 5. Fluorescence spectra for the LB films A-*n* and B-*n* excited at 283 nm. The fluorescence intensities are normalized at 338 nm.

spacing layers. As described in the previous part, the PG polymer backbones are preferentially located near the center. This structural property may lead to different r_{DA} between A-*n* and B-*n*, because the backbone is "labeled" with chromophores in the present system. In the next section, computer simulations are performed to obtain quantitative understanding of this system.

Theoretical Calculations of Transfer Efficiency. For the computer simulations, the structural model based on the result of X-ray measurements was employed. As schematically shown in Figure 6a, the rods bearing D or A molecules are arranged in the matrix of alkyl side chains. The rodlike main chains in a bilayer are interdigitated closely, and the thickness of interdigitated backbones was determined to be 1.9 nm by X-ray reflectometry in the previous study.[16] The radius of the rod's core was also determined to be 0.28 nm by X-ray diffraction.[27,28] Applying these values to the model, the distances between the center of the rods in D and A layers (named as *r*) were determined as summarized in Table 3.

At first, donor (D) or acceptor (A) molecules are placed around the rod in the chromophoric layer using random numbers, while keeping the radius of 0.7 nm, which is approximately measured from the molecular model.

The Förster theory for the energy transfer by the dipole−dipole interaction gives the following rate equation[29]

$$k_T = \frac{1}{\tau_0}\left(\frac{r_0}{r_{DA}}\right)^6 \tag{1}$$

where k_T is the energy transfer rate from an excited D to A, r_{DA} is the distance between D and A, τ_0 is the lifetime of D, and r_0 is the Förster radius of D−A pair. These parameters for naphthalene and anthracene pair were obtained as $r_0 = 2.31$ nm and $\tau_0 = 37$ ns.

According to eq 1, the transfer rate from a certain donor *i* to an acceptor *j* is given by

$$k_{T_{ij}} = \frac{1}{\tau_0}\left(\frac{r_0}{r_{ij}}\right)^6 \tag{2}$$

where r_{ij} is the distance of separation between *i* and *j*. Since the excitation energy of the donor can transfer to all acceptors, the rate must be presented by the sum of eq 2

$$k_{T_i} = \frac{1}{\tau_0}\sum_j\left(\frac{r_0}{r_{ij}}\right)^6 \tag{3}$$

The survival probability p_i of the excited donor *i* at a time *t* is calculated as follows:

$$p_i(t) = \exp\left(-\frac{t}{\tau_0} - k_{T_i}t\right) \tag{4}$$

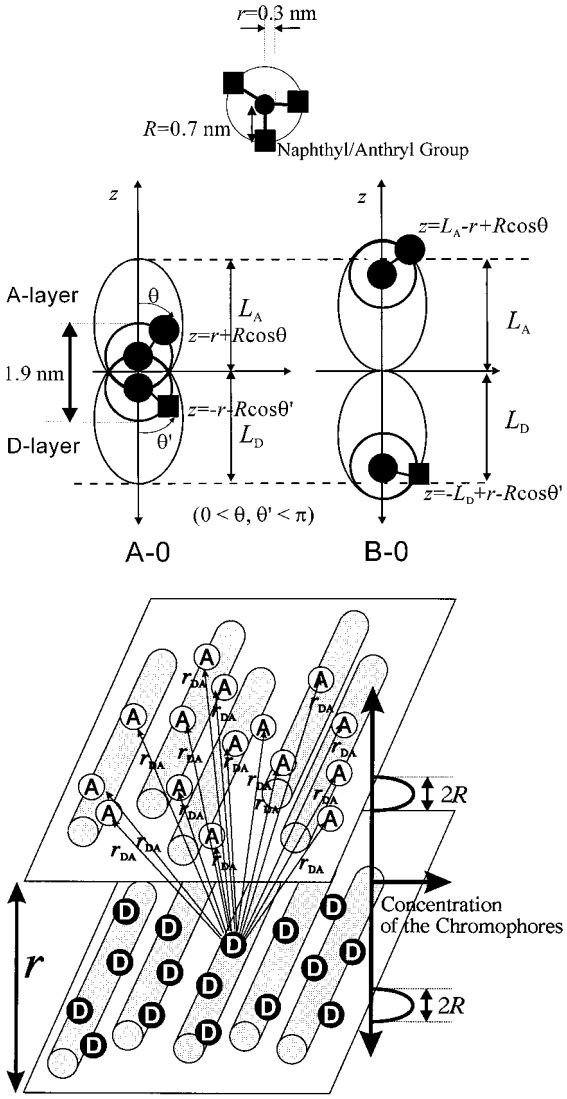

Figure 6. (a) Schematic illustration of the distribution of the chromophores in the adjacent D and A layers. (b) Schematic illustration of the multilayer model used for the simulation. The letter *r* in the figure indicates the distance between the center of the D-labeled rod and the center of the A-labeled rod. D and A denote the donor and acceptor molecules, respectively.

Table 3. Distance between the Center of the Rods Labeled with Donor and Acceptor

sample	*r* (nm)[a]
A-0	0.56
B-0	$L_D + L_A - 0.56$
A-2	$2L + 0.56$
B-2	$2L + L_D + L_A - 0.56$

[a] *L*, L_D, and L_A are the monolayer thickness of PG, PG−Np, and PG−An, respectively, which are listed in Table 2.

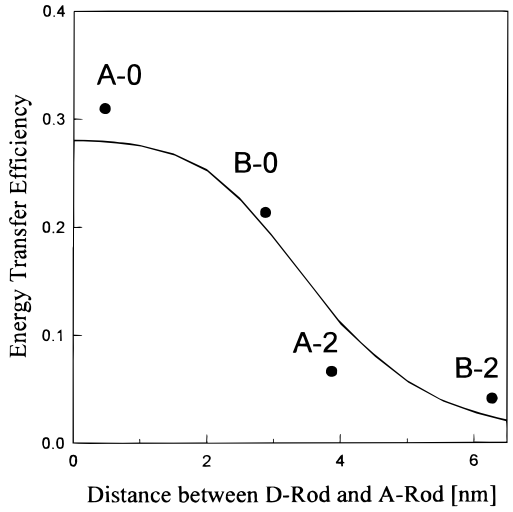

Figure 7. Plot of measured energy transfer efficiency against *r*, the distance between Np-labeled rod and An-labeled rod. The solid line shows the theoretical curve by the simulation.

The observed $p(t)$ for the system, which corresponds to the fluorescence decay curve, is given by the average of $p_i(t)$ over all donor molecules.

$$p(t) = \frac{1}{n_D}\sum_i p_i(t) \tag{5}$$

where n_D is the number of donors. Integration of eq 5 gives the fluorescence quantum yield q_D of the donor under the steady-state excitation.

$$q_D = k_f \int_0^\infty p(t)\, dt \tag{6}$$

where k_f is the emission probability of the excited donor. Therefore, the energy transfer efficiency T_e is evaluated by

$$T_e = \frac{q_{D0} - q_D}{q_{D0}} \tag{7}$$

where q_{D0} is the quantum efficiency of donor without energy transfer.

All of these eqs 2−7 are numerically calculated for a given distribution of D and A chromophores as shown in Figure 6b. This procedure is repeated at least 100 times, and then the averaged efficiency is employed as a theoretical prediction of the energy transfer efficiency. These calculations were performed in an area of 20 × 20 nm^2, which is large enough to be compared with the Förster radius, r_0.

Figure 7 shows the plot of measured transfer efficiency and the theoretical efficiency curve as a function of the distance of separation. The experimental data of the transfer efficiency were successfully plotted along the theoretical curve based on the present model. This result ensures the validity of the assumption for the layered structure where the chromophores are arranged within a limited space in the monolayer by the rigidity of the main chain.

Thermal Stability of the Layered Structure at Temperatures below 100 °C. The energy transfer method was also used to measure the thermal stability of the layered structure. Molecular dynamics of the PG LB films at low temperatures has been studied by dielectric spectroscopy[30,31] and solid-state NMR spectroscopy,[32,33] and their relaxation has been discussed from the view of the elements of chemical structure. However, thermal stability around/above room temperature is more important for application to devices. The thermal stability of the PG multilayer structure has been investigated by X-ray reflectometry and neutron reflectometry,[16,17] but the fluorescence method provides another approach for monitoring the multilayer stability in nanometer dimensions. As a measure of the energy transfer efficiency, the intensity ratio I_A/I_D was employed, where I_A and I_D are the fluorescence intensities at 415 nm (from An emission) and 338 nm (from Np emission), respectively. The change of I_A/I_D in the first course of heating was measured against the temperature, which is shown in Figure 8a. Apparently, the change of I_A/I_D by the thermal treatment was small, revealing the excellent thermal stability of the layered structure for the PG LB films. The stability was much higher than that for the LB films of low molecular weight fatty acids[34] or other polymers with a flexible main chain.[35,36]

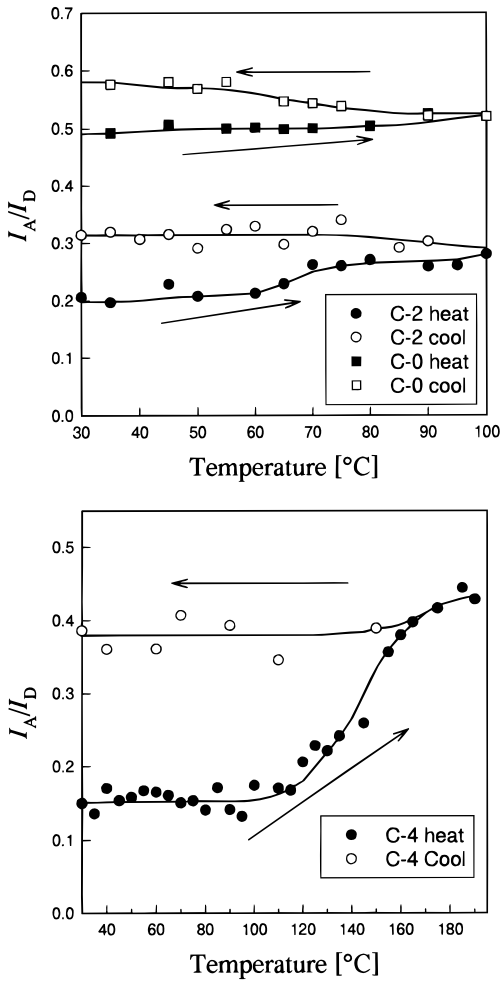

Figure 8. (a) Effect of heating/cooling on the I_A/I_D for the C-*n* LB films up to 100 °C. Filled symbols indicate the values on the heating process, and open ones indicate the cooling process. (b) Effect of heating/cooling on the I_A/I_D for C-4 up to 190 °C. Filled symbols indicate the values on the heating process, and open ones indicate the cooling process.

In general, polymeric LB films, most of which are made of polymers with a flexible main chain, are more stable than those of low molecular weight amphiphilic compounds. However, at temperatures above T_g, the

segmental motion of the polymer main chain becomes active, giving rise to relaxation of the multilayered structure.[35] This process is mostly governed by the "entropy relaxation" from a 2-dimensional conformation to a 3-dimensional random coil state.[37] On the contrary, in the PG LB films, the α-helical structure of the polyglutamate chain which is stabilized by hydrogen bonds makes the macromolecules behave like a rigid rod. This rigid structure restrains the segmental motion of the polymer main chains; therefore, the layered structure is kept stable.

A slight increase observed for both C-0 and C-2 is probably due to the relaxation of the noncentered structure in the monolayers. Since the melting temperature of the alkyl side chain is approximately 40 °C,[13a] the rodlike main chain has a mobility in the liquidlike matrix of the side chain at higher temperatures. At these temperatures, the noncentered structure of "hairy-rod" is likely to change to an equilibrium state where the rod's position shifts to the center of each layer; the Np-labeled rods of the upper layer and the An-labeled rods of the lower layer come closer, yielding a slight increase of transfer efficiency. This is supported by the finding obtained by X-ray reflectometry that the Bragg peak which shows that the periodic bilayered structure diminished after annealing at around 80 °C.[8,13,16,17]

Thermal Stability of the Layered Structure at Temperatures above 100 °C. It was difficult to detect well-resolved fluorescence spectra at temperatures higher than 100 °C because of the thermal quenching of the emission and the broadening of the spectra. Another problem was the damage of the fluorescent probe. After heating the films of PG−Np and PG−An at 200 °C for 2 h, about 20% of chromophores were degraded in both samples, but the ratio I_A/I_D was not affected by the thermal treatment in the range of experimental error less than 5%. Thus, it is not necessary to care about this effect so long as the I_A/I_D is used as a measure of disordering of the layered structure.

Next, in situ observation of I_A/I_D was attempted up to 190 °C. As shown in Figure 8b, the I_A/I_D for C-4 starts increasing at around 120 °C and then became almost constant in the further heating/cooling process. This means that the disordering occurs in this temperature range. The values of I_A/I_D for C-*n* after the treatment at 160 °C for 2 h were around 0.4−0.5 regardless of the number of spacing layers, *n*. These values are in good agreement with the calculated value for the film in which all the main chains are homogeneously dispersed. From these results it can be concluded that the layered structure is irreversibly disordered at 160 °C to the equilibrium state in which PG rods are randomly mixed.

Figure 9 shows the IR spectra taken at room temperature before/after the annealing at 200 °C. The spectra did not show any appreciable shift for the amide I band at 1655 cm^{-1}, amide II band at 1556 cm^{-1}, and amide V band at 620 cm^{-1}, all of which are typical for α-helix, indicating that the PG chains keep the α-helical conformation before/after the annealing. Similar results were obtained for the LB films of PG−Np or PG−An.

Kajiyama et al. reported from the viscoelastic measurement that there were several relaxation modes of poly(γ-alkyl-D-glutamate)s, and they are labeled as α, β, γ, etc., on the order of decreasing temperature.[38] The α relaxation is assigned to the molecular motion of the polymer main chain around 180−200 °C. The β relaxation around 120−130 °C arises from micro-Brownian

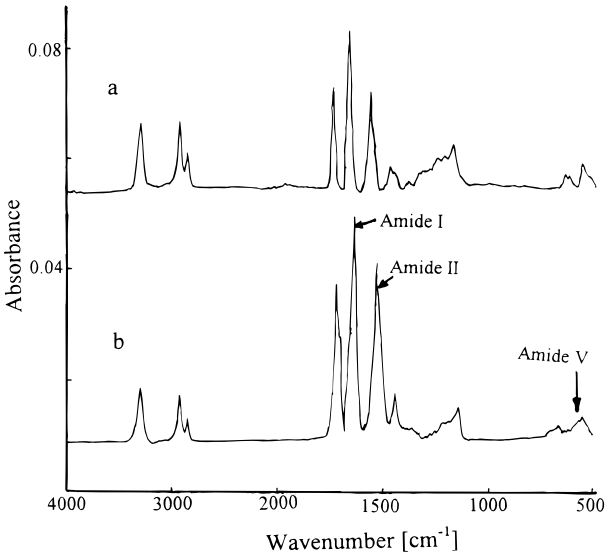

Figure 9. IR spectra for the PG 31-layer LB film before (a) and after (b) annealing at 200 °C.

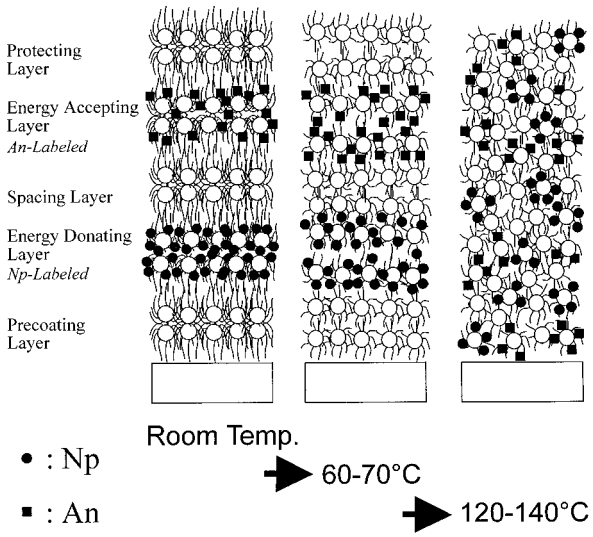

Figure 10. Schematic presentation of thermal relaxation for the PG LB film.

segmental motion of the disordered region or the distorted part of the α-helices. The other relaxation modes below 100 °C are related to the local side chain motion on a small scale. The disordering in the present case may be closely related to these relaxation modes. These relaxation processes are schematically summarized in Figure 10. The layered structure is kept stable up to at least 100 °C although the noncentered structure of each layer may relax. At temperatures higher than 120 °C, the layered structure is disordered to an equilibrium state in which the α-helical backbones are randomly distributed.

Conclusion

The nanostructure of the hairy-rod polymer LB films was characterized by means of X-ray analysis and the fluorescence method. The fluorescent probes introduced around the stiff main chain provide information on the location of the main chain in the multilayered films. The energy transfer rate could be controlled by changing the sequence of deposition. Particularly, when the number of precoating layers (odd or even) was altered, the

transfer efficiency was changed even if the energy-donating layer and the energy-accepting layer were separated by the same number of spacing layers. This effect comes from the noncentered structure of each layer in which the stiff main chains are located away from the center of the layer. The thermal stability of multilayers was also investigated by monitoring the change of the energy transfer efficiency. The rigid structure of the α-helix restrains the segmental motion of polymer chains, giving a stable layered structure, although the layer structure was disordered at a temperature higher than 120 °C. Thus, PG can be used to arrange guest molecule around the main chain, providing thermally stable ultrathin films having particular molecular architectures.

Acknowledgment. This work was supported by a Grant-in-Aid for Scientific Research on Priority Areas (No. 09241216) from the Ministry of Education, Science, Sports and Culture of Japan and by a fellowship to M. Mabuchi from the Schlössmann Foundation through the Max-Planck Society.

References and Notes

(1) (a) Tredgold, R. H.; Winter, C. S. *J. Phys. D.: Appl. Phys.* **1982**, *15*, L55. (b) Tredgold, R. H.; Winter, C. S. *Thin Solid Films* **1983**, *99*, 81. (c) Winter, C. S.; Tredgold, R. H. *Thin Solid Films* **1985**, *125*, L1. (d) Tredgold, R. H. *Thin Solid Films* **1987**, *152*, 223.
(2) Embs, F.; Funhoff, D.; Laschewski, A.; Licht, U.; Ohst, H.; Prass, W.; Ringsdorf, H.; Wegner, G.; Wehrmann, R. *Adv. Mater.* **1991**, *3*, 25.
(3) Breton, T. *J. Macromol. Sci. Rev. Chem.* **1995**, *C21*, 1326.
(4) Miyashita, M. *Prog. Polym. Sci.* **1993**, *18*, 263.
(5) Kakimoto, M.; Suzuki, M.; Konishi, T.; Imai, Y.; Iwamoto, M.; Hino, T. *Chem. Lett.* **1986**, 823.
(6) (a) Ohmori, S.;. Ito, S.; Yamamoto, M.; Yonezawa, Y.; Hada, H. *J. Chem. Soc., Chem. Commun.* **1989**, 1293. (b) Ohmori, S.; Ito, S.; Yamamoto, M. *Macromolecules* **1991**, *24*, 2377. (c) Ito, S.; Okubo, H.; Ohmori, S.; Yamamoto, M. *Thin Solid Films* **1989**, *179*, 445.
(7) Wegner, G. *Thin Solid Films* **1992**, *216*, 105.
(8) Wegner, G. *Mol. Cryst. Liq. Cryst.* **1993**, *235*, 1.
(9) Friedenberg, M. C.; Fuller, G. C.; Frank, C. W.; Robertson, C. R. *Macromolecules* **1996**, *29*, 705.
(10) Schwiegk, S.; Vahlenkamp, T.; Xu, Y.; Wegner, G. *Macromolecules* **1992**, *25*, 2513.
(11) (a) Lee, S.; Dutcher, I. R.; Hillebrands, B.; Stegeman, G. I.; Knoll, W.; Duda, G.; Wegner, G. *Mater. Res. Soc. Symp. Proc.* **1990**, *188*, 355. (b) Nizzolim, F.; Hillebrands, B.; Lee, S.; Stegeman, G. I.; Duda, G.; Wegner, G.; Knoll, W. *Mater. Sci. Eng.* **1990**, *B5*, 173.
(12) (a) Duda, G.; Schouten, A. J.; Arndt, T.; Lieser, G.; Schmidt, G. F.; Bubeck, C.; Wegner, G. *Thin Solid Films* **1988**, *159*, 221. (b) Duda, G. Ph.D. Thesis, University of Mainz, Mainz, Germany, 1988.
(13) (a) Menzel, H.; Hallensleben, M. L. *Polym. Bull.* **1991**, *27*, 89. (b) Menzel, H.; Weichart, B.; Hallensleben, M. L. *Thin Solid Films* **1993**, *223*, 181. (c) Menzel, H.; Weichart, B.; Schmidt, A.; Paul, S.; Knoll, W.; Stumpe, J.; Fischer, T. *Langmuir* **1994**, *10*, 1926.
(14) Bücher, H.; Drexhage, K. H.; Fleck, M.; Kuhn, H.; Möbius, D.; Schäfer, F. P.; Sondermann, J.; Sperling, W.; Tillmann, P.; Wiegand, J. *Mol. Cryst.* **1967**, *2*, 199.
(15) Kuhn, H.; Möbius, D.; Bücher, H. In *Physical Methods of Chemistry*; Weissberger, A., Rossiter, B. W., Eds.; Wiley: New York, 1972; Vol. 1, Part 3B, p 557.
(16) Vierheller, T. R.; Foster, M. D.; Schmidt, A.; Mathauer, K.; Knoll, W.; Wegner, G.; Satija, S.; Majkrzak, C. F. *Macromolecules* **1994**, *27*, 6893.
(17) Schmidt, A.; Mathauer, K.; Reiter, G.; Foster, M. D.; Stamm, M.; Wegner, G.; Knoll, W. *Langmuir* **1994**, *10*, 3280.
(18) Mabuchi, M.; Kobata, S.; Ito, S.; Yamamoto, M.; Schmidt, A.; Knoll, W., *Langmuir*, in press.
(19) Some of these samples were difficult to dissolve in pure chloroform and were dissolved in chloroform containing approximately 1% trifluoroacetic acid. Trifluoroacetic acid is one of the helix-breaking solvents; however, it is reported that the main chain of poly(γ-methyl-L-glutamate) is α-helical in the cast film even if prepared from trifluoroacetic acid solution (Hayashi, T. Ph.D. Thesis, Kyoto University, Kyoto, Japan, 1973.). The α-helical conformation in the resultant LB films was confirmed by the CD and FT-IR spectroscopy.[18]
(20) Foster, M.; Stamm, M.; Reiter, R.; Huettenbach, S. *Vacuum* **1990**, *41*, 1441.
(21) Rieutord, F.; Benatter, J. J.; Bosio, L.; Robin, P.; Blot, C.; de Kouchkovsky, R. *J. Phys.* **1987**, *48*, 679.
(22) Rieutord, F.; Benatter, J. J. *Acta Crystallogr.* **1989**, *A45*, 445.
(23) Russell, T. P. *Mater. Sci. Rep.* **1990**, *5*, 171.
(24) Kiessig, H. *Ann. Phys.* **1931**, *10*, 715.
(25) Malcom, B. R. *Biopolymer* **1966**, *7*, 595.
(26) Berlman, I. B. *Energy Transfer Parameters of Aromatic Compounds*; Academic Press: New York, 1973.
(27) Elliott, A.; Malcolm, B. R. *Proc. R. Soc. London, A* **1958**, *249*, 30.
(28) (a) Pauling, L.; Corey, R. B. *Proc. Nat. Acad. Sci. U.S.A.* **1951**, *37*, 236. (b) Pauling, L.; Corey, R. B. *Proc. Nat. Acad. Sci. U.S.A.* **1951**, *37*, 241.
(29) Förster, Th. *Z. Naturforsch.* **1949**, *4A*, 321.
(30) Blumm, G.; Kremer, F.; Jaworek, T.; Wegner, G. *Adv. Mater.* **1995**, *7*, 1017.
(31) Schmidt, A.; Lehmann, S.; Georgelin, M.; Katana, G.; Mathauer, K.; Kremer, F.; Schmidt-Roher, K.; Boeffel, C.; Wegner, G.; Knoll, W. *Macromolecules* **1995**, *28*, 5487.
(32) (a) Yamaguchi, M.; Tsutsumi, A. *Polym. J.* **1990**, *22*, 781. (b) Yamaguchi, M.; Tsutsumi, A. *Polym. J.* **1993**, *25*, 131.
(33) Romeo Colomer, J.; Gómez Ribelles, J. L.; Barrales-Rienda, J. M. *Macromolecules* **1994**, *27*, 5004.
(34) Hayashi, T.; Ito, S.; Yamamoto, M.; Tsujii, Y.; Matsumoto, M.; Miyamoto, T. *Langmuir* **1994**, *10*, 4142.
(35) Ueno, T.; Ito, S.; Ohmori, S.; Onogi, Y.; Yamamoto, M. *Macromolecules* **1992**, *25*, 7150.
(36) Hayashi, T.; Ito, S.; Onogi, Y.; Yamamoto, M.; Matsumoto, A. *Eur. Polym. J.* **1994**, *27*, 2270.
(37) Mabuchi, M.; Kawano, K.; Ito, S.; Yamamoto, M.; Takahashi, M.; Masuda, T. *Macromolecules*, in press.
(38) Kajiyama, C.; Kuroishi, M.; Takayanagi, M. *J. Macromol. Sci., Phys.* **1975**, *B11*, 195.

MA981050F